GEOLOGY | THE GEOLOGICAL SOCIETY OF AMERICA®

https://doi.org/10.1130/G45654.1

Manuscript received 28 September 2018
Revised manuscript received 2 January 2019
Manuscript accepted 4 January 2019

Published online 29 January 2019

© 2019 The Authors. Gold Open Access: This paper is published under the terms of the CC-BY license.

Connection between the Jurassic oceanic lithosphere of the Gulf of Cádiz and the Alboran slab imaged by Sp receiver functions

Antonio Molina-Aguilera[1,2], Flor de Lis Mancilla[1,2], Jose Morales[1,2], Daniel Stich[1,2], Xiaohui Yuan[3], and Benjamin Heit[3]
[1]Instituto Andaluz de Geofisica, Universidad de Granada, Campus de Cartuja, c/Prof. Clavera nº 12, 18071 Granada, Spain
[2]Departamento de Fisica Teorica y del Cosmos, Facultad de Ciencias, Universidad de Granada, Campus de Fuente Nueva, 18071 Granada, Spain
[3]Seismology Section, Helmholtz-Zentrum Potsdam, Deutsches GeoForschungsZentrum, Telegrafenberg, 14473 Potsdam, Germany

ABSTRACT

We investigate the lithospheric structure beneath the Gibraltar arc (western Mediterranean) using S-wave receiver functions (SRFs). From a dense network deployed in the Ibero-Maghrebian region during different seismic surveys, we calculated ~11,000 SRFs that sample the upper mantle detecting the lithosphere-asthenosphere boundary (LAB). The observed seismic LAB belongs to different lithospheric domains: Iberian and African forelands, Alboran domain, and Atlantic Ocean. Common conversion point (CCP) migrated profiles show the geometrical relation among them. Under the Strait of Gibraltar, we observe a deep LAB (~150 km). It can be associated with Jurassic-age lithosphere of ~120 km thickness, one of the thickest ever reported in oceanic environments. There is an abrupt offset between the oceanic LAB and the shallow (80-km-deep) continental LAB of the Iberian foreland, suggesting displacement along a former transform fault. The northwestern African continental LAB is 90–100 km deep. The oceanic LAB under the Gibraltar arc continues to ~180 km depth beneath the Alboran Sea, showing the connection between the Alboran slab and the oceanic lithosphere in the central Gulf of Cádiz. This geometry agrees with an ~200-km-wide corridor of oceanic lithosphere between the central Atlantic and the Alpine Tethys, developed during the Middle–Late Jurassic. Our results support the proposed westward rollback of an oceanic east-dipping slab, which has continuity at least to the central Gulf of Cádiz.

INTRODUCTION

The southern Iberian Peninsula and the western Maghreb include a sector of the Nubia-Eurasia plate boundary zone that is characterized by complex tectonics, widespread deformation, and the interaction between continental and oceanic domains. At the center of this region, the Strait of Gibraltar separates the Atlantic Ocean (Gulf of Cádiz) from the Mediterranean (Alboran Sea), and at the same time connects the Alpine mountain ranges in Iberia (Betics) to Africa (Rif). The present-day configuration, with the characteristic tightly curved orogenic arc (Fig. 1), results mainly from the interplay between slow, northwest-southeast convergence between Eurasia and Nubia and fast westward slab retreat since the Miocene (e.g., Lonergan and White, 1997; Spakman and Wortel, 2004; Chertova et al. 2014). The complexity of the Iberia-Maghreb plate-boundary zone has been represented with increasing detail as more and more observational data from different disciplines have become available. Yet, fundamental aspects of the geodynamics and lithospheric structure are still discussed controversially (e.g., Gutscher et al., 2012; Mancilla et al., 2013).

The Alboran slab is a key element for understanding regional geodynamics. Together with the Calabrian slab, these structures represent the present configuration of the western Mediterranean subduction system, involving the cold oceanic lithosphere of the Alpine Tethys (e.g., Lonergan and White, 1997; van Hinsbergen et al., 2014). While the Calabrian subduction remains clearly active today, with associated seismicity, active volcanism, and an active accretionary wedge (e.g., Gutscher et al., 2017; Scarfi et al., 2018), there is a lack of evidence for ongoing subduction of the Alboran slab. Deep and intermediate-depth earthquakes do not depict a continuous Wadati-Benioff zone (e.g., Buforn et al., 1991; Heit et al., 2017). Earthquake focal mechanisms, the stress field, and geodetic deformation (e.g., Stich et al., 2006) reflect Nubia-Eurasia plate motion rather than subduction dynamics. Furthermore, absolute plate motions appear to have strong influence on the current slab dynamics (Spakman et al., 2018).

The Alboran slab has been imaged clearly by recent tomographic inversions as a subvertical high-velocity anomaly beneath the western Alboran Sea and southern Spain. However, its possible connection to the oceanic lithosphere west of Gibraltar remains debated (e.g., Spakman and Wortel, 2004; Bezada et al., 2013). The variability in the geoid height in the region (Fig. 1) points to relevant topography of the lithosphere-asthenosphere boundary (LAB) in the region. In this study, we map the depth of the seismic LAB from S-wave receiver functions (SRFs), showing the conversions of teleseismic S-to-P waves at the LAB discontinuity. The analysis builds upon several seismic deployments during the last decade (Fig. 1B), which allows for broad coverage of the LAB over the region, and favors the use of stacking techniques to enhance the LAB signals. We attempt to increase frequency range and spatial resolution compared to previous SRF studies (Miller et al., 2015) in order to shed more light on the interaction of the subduction system with the surrounding lithosphere.

DATA AND METHOD

We analyze S-to-P conversions of teleseismic earthquakes (SRFs) recorded at a dense network of ~300 permanent and temporary seismic stations in Iberia and Morocco (Fig. 1B). This corresponds to an average interstation distance of ~60 km over most of the area and ~30 km locally. SRF analysis is a particularly suitable approach to study deep

CITATION: Molina-Aguilera, A., et al., 2019, Connection between the Jurassic oceanic lithosphere of the Gulf of Cádiz and the Alboran slab imaged by Sp receiver functions: Geology, v. 47, p. 227–230, https://doi.org/10.1130/G45654.1.

Downloaded from https://pubs.geoscienceworld.org/gsa/geology/article-pdf/47/3/227/4650237/227.pdf
by Univ de Granada Biblioteca Fac de Ciencias user

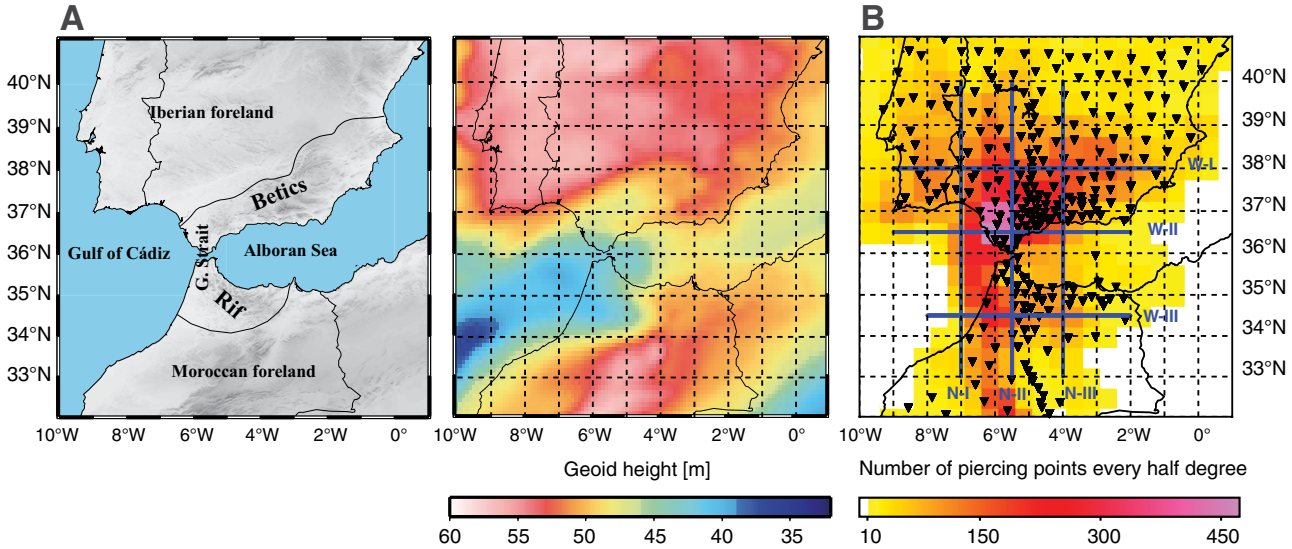

Figure 1. A: Shaded-relief map and geoid height of Gibraltar arc area (global model EGM2008 with WGS84 reference ellipsoid: Pavlis et al., 2012; retrieved from the International Centre for Global Earth Models [ICGEM] at GeoForschungsZentrum–Potsdam, Germany). G. Strait—Strait of Gibraltar. B: Distribution of seismic stations (inverted triangles) and piercing points at 100 km depth (colored contours). Blue lines mark common conversion point profiles shown in Figure 2.

lithospheric structures. S-to-P conversions arrive before the direct onset, thus avoiding the interference of LAB converted signals with crustal reverberations, common in P-to-S receiver functions (PRFs; e.g., Yuan et al., 2006). Furthermore, SRF analysis permits sampling larger areas compared to PRFs, due to the larger incidence angle of S-waves. This allows for better coverage in offshore areas because the piercing points of SRFs are located farther away from the stations (Fig. 1B).

We use teleseismic events with magnitude M_b >5.8 within the epicentral distance range of 65°–85°. We include in the analysis all of the available seismograms with signal-to-noise ratio >2.5, and rotate the three-component records into the ZRT (vertical, radial, transverse) coordinate system using theoretical back-azimuth angles. Following, a rotation into ray-based longitudinal, radial, transverse (LQT) coordinates is done, minimizing the SV-wave energy on the Q component at the theoretical S-wave onset. We time-reverse the traces about the S-wave onset in order to analyze the SRF in the precursor time window, only affected by the primary S-to-P conversions.

Prior to deconvolution, we use a band-pass filter from 1 to 30 s. We apply a time-domain deconvolution method of the SV component (Q component) from the vertical component (L component) using the iterative deconvolution method developed by Ligorría and Ammon (1999) with a 2-s-wide Gaussian basis function. A 6 s low-pass filter is applied after deconvolution to enhance the LAB conversion. We obtain ~11,000 individual SRFs (Fig. DR1 in the GSA Data Repository[1]). The LAB can be identified by the prominent negative signal (blue color) after the Moho conversion, at 15–20 s travel time.

Piercing points at 100 km depth show a dense distribution, including offshore areas in the Alboran Sea and Gulf of Cádiz (Fig. 1B). This enables us to build cross-sections by stacking SRF amplitudes applying a common conversion point (CCP) approach (e.g., Mancilla et al., 2015). We consider single scattering, taking into account the first Fresnel zone, for back-projection of SRFs in the IASP91 velocity model (Kennett and Engdahl, 1991). We build north-south and west-east cross-sections by stacking all receiver-function amplitudes with piercing points within 1° distance at both sides of each profile (Fig. 2). We apply a binning of 5 × 5 km^2; bins with fewer than 10 samples are not taken into account.

[1]GSA Data Repository item 2019084, raw S-wave receiver functions, is available online at http://www.geosociety.org/datarepository/2019/, or on request from editing@geosociety.org.

RESULTS AND DISCUSSION

Migrated profiles show clear and coherent signals. Two principal signals can be recognized in all cross-sections. The shallower signal corresponds to a positive conversion (increasing velocity with depth) within the first 60 km, attributed to the Moho discontinuity. Within the resolution of SRFs (>10 km), the lateral variations of the Moho topography in this study agree with previous PRF observations (e.g., Mancilla and Diaz, 2015). The deeper signal corresponds to a negative velocity contrast at depths between 50 and 180 km. This signal is interpreted as the seismic LAB discontinuity.

Common conversion point (CCP) sections across the Iberian massif show a relatively flat LAB located at 80–90 km depth (IBL in Fig. 2, profile W-I). Similar lithospheric thickness has already been reported by previous tomographic (e.g., Palomeras et al., 2017), PRF (Mancilla et al., 2015), and SRF (Miller et al., 2015) studies. This shallow LAB discontinuity has been attributed to a large-scale delamination of thickened continental lithosphere of the Variscan belts in Europe during middle Permian time (e.g., Gutiérrez-Alonso et al., 2011).

In northern Morocco, a west-east profile shows relatively large topographic variations in the LAB (Fig. 2, profile W-III). An offset of ~40 km occurs near 4°W longitude from 100 km depth under the Rif mountains to 60–50 km depth near the Nekor fault to the east. This observation agrees with previous studies that reported strong crustal and lithospheric thickness contrasts in the area, coincident with the intersection between the Trans-Alboran shear zone and the Moroccan margin (e.g., Gil et al., 2014; Miller et al., 2015).

The largest variations in the topography of the LAB discontinuity are observed beneath the Strait of Gibraltar and Gulf of Cádiz. The CCP profiles reveal two different negative converters (Fig. 2, profiles W-II, N-I, and N-II). The shallower one has depths of 80–90 km and represents the Iberian LAB (IBL in Fig. 2). The deeper signal emerges at 8°W at ~150 km depth (Fig. 2, profile W-II), starts deepening eastward under the Strait of Gibraltar (~6.5°W), reaching ~180 km depth at ~5°W beneath the Alboran Sea (JOL in Fig. 2, profile W-II). By 4°W, the oceanic LAB (JOL) has disappeared completely, and a shallow LAB at 50 km depth emerges eastern side of the profile W-II (Fig. 2), corresponding to the thinned continental Alboran lithosphere, already imaged in previous studies (ALL in Fig. 2, profile N-III; e.g., Mancilla et al., 2015; Heit et al., 2017). The western termination of the oceanic LAB signal (JOL) can be attributed to the lack of data coverage beyond 8°W (Fig. 1).

Downloaded from https://pubs.geoscienceworld.org/gsa/geology/article-pdf/47/3/227/4650237/227.pdf
by Univ de Granada Biblioteca Fac de Ciencias user

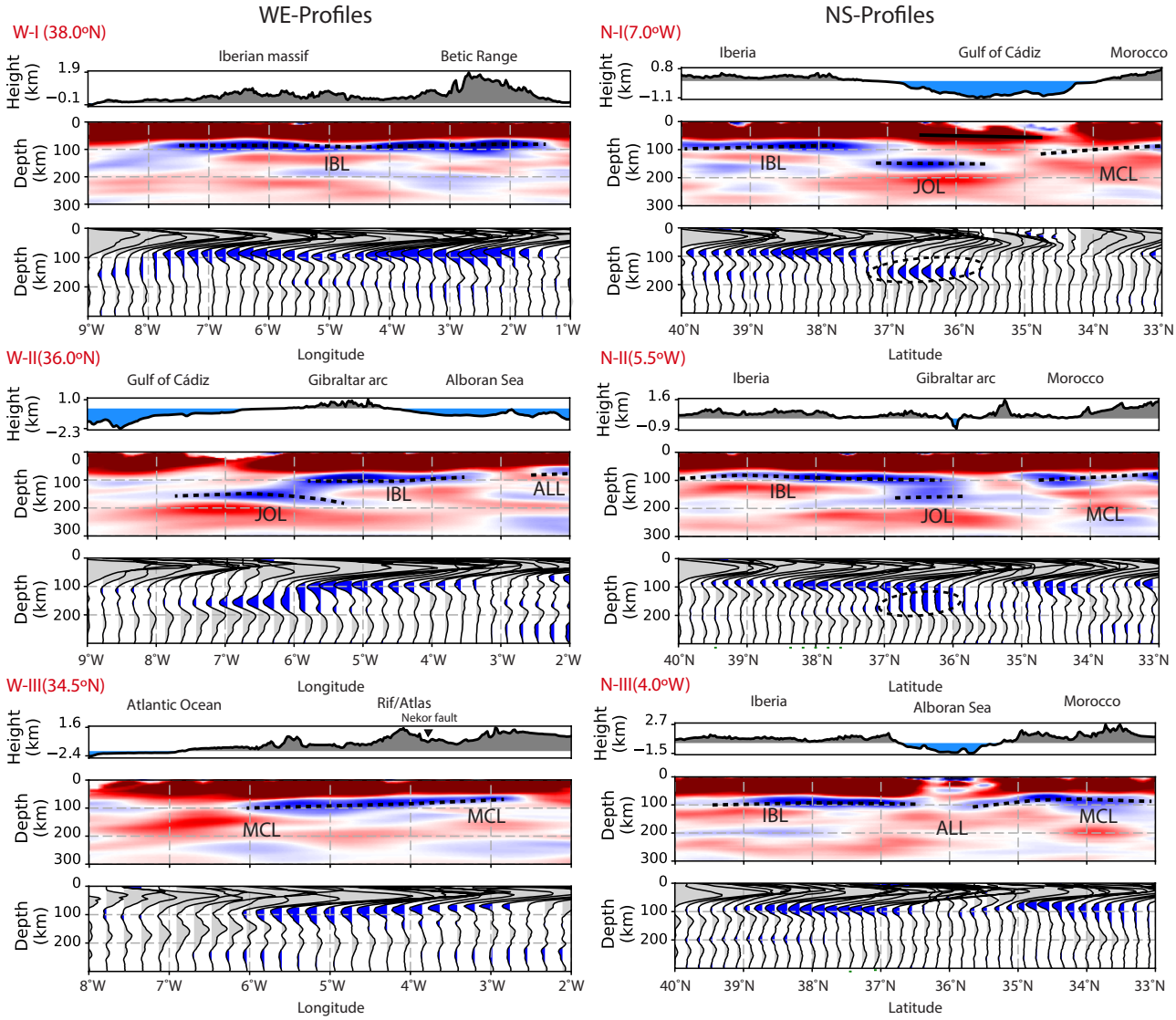

Figure 2. Common conversion point profiles in west-east (left) and north-south (right) directions (see Fig. 1 for location); red indicates positive and blue indicates negative amplitudes. For reference, we show topography along profiles. For consistency among different cross-sections, we use same normalization for all profiles. Lower panels show stacked traces derived directly from migrated images. Dashed black lines delineate lithosphere-asthenosphere boundary (LAB) discontinuity along different domains: Alboran (ALL), Moroccan (MCL), Iberian (IBL), and Jurassic oceanic corridor (JOL).

We associate the deeper negative velocity contrast (JOL in Fig. 2, profile W-II), under the Alboran Sea, to the LAB discontinuity of the Alboran slab observed in tomography studies (e.g., Spakman and Wortel, 2004; Bezada et al., 2013, Palomeras et al., 2017). The eastern termination of the LAB signal (~5°W; Fig. 2, profile W-II) agrees with the location where the Alboran slab starts subducting nearly vertically, impeding detection by S-to-P conversions (Li et al., 2011). Our results show the continuity of the LAB discontinuity from Alboran slab oceanic lithosphere across the Strait of Gibraltar to the Gulf of Cádiz (JOL in Fig. 2, profile W-II). This allows for connecting the Alboran slab with the oceanic crust detected in the Gulf of Cádiz (Sallarès et al., 2011), providing direct evidence for the presence of a corridor of oceanic lithosphere beneath the Strait of Gibraltar. This corridor has been inferred by paleogeographic reconstructions to be Jurassic-age oceanic materials connecting the Alpine Tethys with the central Atlantic Ocean (Frizon de Lamotte et al., 2011; Stampfli and Borel, 2002). The extent of the oceanic LAB along cross-section N-I (Fig. 2) shows a good match with the geoid low under the Strait of Gibraltar (Fig. 1).

The apparent width of the oceanic corridor can be estimated as ~200 km in the north-south profiles (Fig. 2, profile N-I). To the north, the flat oceanic LAB is limited by an offset of ~70 km with respect to the Iberian continental LAB at ~37°N. This lithospheric offset may be related to a prior transform fault, in agreement with the sharp transition between continental and oceanic crust observed by Sallarès et al. (2011) and with the location and focal mechanisms of subcrustal earthquakes (Stich et al., 2005) possibly associated with this structure. This observation is supported, too, by CCP images of PRFs along a similar north-south profile (Mancilla et al., 2015). The PRF profiles image Moho offsets of roughly 6–9 km under the Strait of Gibraltar, in agreement with the expected thickness of oceanic crust (Mancilla et al., 2015). The apparent overlap of the Iberian continental and oceanic LABs in profile N-II (Fig. 2) is likely an artifact due to the projection of independent structures within 1° at both sides of the profile. To the south, the transition to the African foreland LAB is imaged less abruptly at ~35°N.

The observed LAB depth of the oceanic corridor is unusually large in a global comparison (e.g., Rychert and Harmon, 2018). The thickness of oceanic lithosphere depends on age and is currently explained by two competing models: a half-space cooling model (HSC; Stein and Stein, 1992) and a plate model (PM; Grose and Afonso, 2013). They differ for

Downloaded from https://pubs.geoscienceworld.org/gsa/geology/article-pdf/47/3/227/4650237/227.pdf
by Univ de Granada Biblioteca Fac de Ciencias user

ages >70 Ma. The oceanic lithosphere in the Gulf of Cádiz is from the Middle to Late Jurassic (>145 Ma, e.g., Stampfli and Borel, 2002), among the oldest not yet consumed by subduction. For these ages, PM predicts a lithospheric thickness of slightly less than 100 km, and HSC predicts values of ~110–130 km (Rychert and Harmon, 2018). The observed LAB of the oceanic corridor supports the HSC model. The remaining difference can be attributed to the presence of ~30 km of overriding Alboran domain crust on top of the oceanic lithosphere at the Strait of Gibraltar.

CONCLUSIONS

The analysis of a large number of SRFs (~11,000) has revealed the topography of the seismic LAB discontinuity beneath the complex plate-boundary zone between Iberia and northern Africa. Four different domains can be clearly distinguished, some of them limited by sharp vertical offsets. We confirm previous LAB depth estimates for the Iberian and Moroccan forelands. Under the Alboran domain, we find a thin lithosphere of 50–60 km thickness. The largest LAB depths are observed under the Strait of Gibraltar, outlining an ~200-km-wide corridor of Middle to Late Jurassic lithosphere with ~120 km thickness, being one of the thickest oceanic lithospheres ever detected. The main conclusion that emerged from the CCP images is the clear spatial connection between the Alboran slab under the Alboran Sea and the Atlantic oceanic crust through this oceanic corridor below the Gulf of Cádiz.

ACKNOWLEDGMENTS

We are grateful to the staff involved in the Topo-Iberia, Picasso, Indalo, and Hire projects and the Instituto Andaluz de Geofísica and Instituto Geográfico Nacional permanent networks. A. Molina-Aguilera acknowledges Felix M. Schneider for helping him at the beginning with SRF methodology. We thank W. Spakman and the editor D. Brown for their comments. This work was supported by the Spanish national projects CGL2015-67130-C2-2-R/FEDER and CGL2012-31472. We acknowledge work on free software SAC and GMT.

REFERENCES CITED

Bezada, M.J., Humphreys, E.D., Toomey, D.R., Harnafi, M., Dávila, J.M., and Gallart, J., 2013, Evidence for slab rollback in westernmost Mediterranean from improved upper mantle imaging: Earth and Planetary Science Letters, v. 368, p. 51–60, https://doi.org/10.1016/j.epsl.2013.02.024.

Buforn, E., Udias, A., and Madariaga, R., 1991, Intermediate and deep earthquakes in Spain: Pure and Applied Geophysics, v. 136, p. 375–393, https://doi.org/10.1007/BF00878576.

Chertova, M.V., Spakman, W., Geenen, T., van den Berg, A.P., and van Hinsbergen, D.J.J., 2014, Underpinning tectonic reconstructions of the western Mediterranean region with dynamic slab evolution from 3-D numerical modeling: Journal of Geophysical Research: Solid Earth, v. 119, p. 5876–5902, https://doi.org/10.1002/2014JB011150.

Frizon de Lamotte, D., Raulin, C., Moucho, N., Wrobel-Daveau, J.-C., Blanpied, C., and Ringenbach, J.-C., 2011, The southernmost margin of the Tethys realm during the Mesozoic and Cenozoic: Initial geometry and timing of the inversion processes: Tectonics, v. 30, TC3002, https://doi.org/10.1029/2010TC002691.

Gil, A., Gallart, J., Díaz, J., Carbonell, R., Torné, M., Levander, A., and Harnafi, M., 2014, Crustal structure beneath the Rif Cordillera, North Morocco, from the RIFSIS wide-angle reflection seismic experiment: Geochemistry Geophysics Geosystems, v. 15, p. 4712–4733, https://doi.org/10.1002/2014GC005485.

Grose, C.J., and Afonso, J.C., 2013, Comprehensive plate models for the thermal evolution of oceanic lithosphere: Geochemistry Geophysics Geosystems, v. 14, p. 3751–3778, https://doi.org/10.1002/ggge.20232.

Gutiérrez-Alonso, G., Murphy, J.B., Fernández-Suárez, J., Weil, A.B., Franco, M.P., and Gonzalo, J.C., 2011, Lithospheric delamination in the core of Pangea: Sm-Nd insights from the Iberian mantle: Geology, v. 39, p. 155–158, https://doi.org/10.1130/G31468.1.

Gutscher, M.-A., et al., 2012, The Gibraltar subduction: A decade of new geophysical data: Tectonophysics, v. 574–575, p. 72–91,, https://doi.org/10.1016/j.tecto.2012.08.038 .

Gutscher, M.-A., et al., 2017, Active tectonics of the Calabrian subduction revealed by new multi-beam bathymetric data and high-resolution seismic profiles in the Ionian Sea (Central Mediterranean): Earth and Planetary Science Letters, v. 461, p. 61–72, https://doi.org/10.1016/j.epsl.2016.12.020.

Heit, B., Mancilla, F., Yuan, X., Morales, J., Stich, D., Martín, R., and Molina-Aguilera, A., 2017, Tearing of the mantle lithosphere along the intermediate-depth seismicity zone beneath the Gibraltar Arc: The onset of lithospheric delamination: Geophysical Research Letters, v. 44, p. 4027–4035, https://doi.org/10.1002/2017GL073358.

Kennett, B.L.N., and Engdahl, E.R., 1991, Travel times for global earthquake location and phase association: Geophysical Journal International, v. 105, p. 429–465.

Li, X., Wei, D., Yuan, X., Kind, R., Kumar, P., and Zhou, H., 2011, Details of the doublet Moho structure beneath Lhasa, Tibet, obtained by comparison of P and S receiver functions: Bulletin of the Seismological Society of America, v. 101, p. 1259–1269, https://doi.org/10.1785/0120100163.

Ligorría, J.P., and Ammon, C.J., 1999, Iterative deconvolution and receiver-function estimation: Bulletin of the Seismological Society of America, v. 89, p. 1395–1400.

Lonergan, L., and White, N., 1997, Origin of the Betic-Rif mountain belt: Tectonics, v. 16, p. 504–522, https://doi.org/10.1029/96TC03937.

Mancilla, F., and Diaz, J., 2015, High resolution Moho topography map beneath Iberia and Northern Morocco from receiver function analysis: Tectonophysics, v. 663, p. 203–211, https://doi.org/10.1016/j.tecto.2015.06.017.

Mancilla, F., Stich, D., Berrocoso, M., Martín, R., Morales, J., Fernández-Ros, A., Páez, R., and Pérez-Peña, A., 2013, Delamination in the Betic Range: Deep structure, seismicity, and GPS motion: Geology, v. 41, p. 307–310, https://doi.org/10.1130/G33733.1.

Mancilla, F., et al., 2015, Crustal thickness and images of the lithospheric discontinuities in the Gibraltar arc and surrounding areas: Geophysical Journal International, v. 203, p. 1804–1820, https://doi.org/10.1093/gji/ggv390.

Miller, M.S., O'Driscoll, L.J., Butcher, A.J., and Thomas, C., 2015, Imaging Canary Island hotspot material beneath the lithosphere of Morocco and southern Spain: Earth and Planetary Science Letters, v. 431, p. 186–194, https://doi.org/10.1016/j.epsl.2015.09.026.

Palomeras, I., Villaseñor, A., Thurner, S., Levander, A., Gallart, J., and Harnafi, M., 2017, Lithospheric structure of Iberia and Morocco using finite-frequency Rayleigh wave tomography from earthquakes and seismic ambient noise: Geochemistry Geophysics Geosystems, v. 18, p. 1824–1840, https://doi.org/10.1002/2016GC006657.

Pavlis, N.K., Holmes, S.A., Kenyon, S.C., and Factor, J.K., 2012, The development and evaluation of the Earth Gravitational Model 2008 (EGM2008): Journal of Geophysical Research, v. 117, B04406, https://doi.org/10.1029/2011JB008916.

Rychert, C.A., and Harmon, N., 2018, Predictions and observations for the oceanic lithosphere from *S*-to-*P* receiver functions and *SS* precursors: Geophysical Research Letters, v. 45, p. 5398–5406, https://doi.org/10.1029/2018GL077675.

Sallarès, V., Gailler, A., Gutscher, M.-A., Graindorge, D., Bartolomé, R., Gràcia, E., Díaz, J., Dañobeitia, J.J., and Zitellini, N., 2011, Seismic evidence for the presence of Jurassic oceanic crust in the central Gulf of Cadiz (SW Iberian margin): Earth and Planetary Science Letters, v. 311, p. 112–123, https://doi.org/10.1016/j.epsl.2011.09.003.

Scarfì, L., Barberi, G., Barreca, G., Cannavò, F., Koulakov, I., and Patanè, D., 2018, Slab narrowing in the Central Mediterranean: The Calabro-Ionian subduction zone as imaged by high resolution seismic tomography: Scientific Reports, v. 8, 5178, https://doi.org/10.1038/s41598-018-23543-8.

Spakman, W., and Wortel, R., 2004, A tomographic view on Western Mediterranean geodynamics, *in* Cavazza, W., et al., eds., The TRANSMED Atlas: The Mediterranean Region from Crust to Mantle: Berlin-Heidelberg, Springer, p. 31–52, https://doi.org/10.1007/978-3-642-18919-7_2.

Spakman, W., Chertova, M.V., van den Berg, A.P., and Hinsbergen, D.J.J., 2018, Puzzling features of western Mediterranean tectonics explained by slab dragging: Nature Geoscience, v. 11, p. 374, https://doi.org/10.1038/s41561-018-0066-z.

Stampfli, G.M., and Borel, G.D., 2002, A plate tectonic model for the Paleozoic and Mesozoic constrained by dynamic plate boundaries and restored synthetic oceanic isochrons: Earth and Planetary Science Letters, v. 196, p. 17–33, https://doi.org/10.1016/S0012-821X(01)00588-X.

Stich, D., Mancilla, F., and Morales, J., 2005, Crust-mantle coupling in the Gulf of Cadiz (SW-Iberia): Geophysical Research Letters, v. 32, L13306, https://doi.org/10.1029/2005GL023098.

Stich, D., Serpelloni, E., Mancilla, F., and Morales, J., 2006, Kinematics of the Iberia-Maghreb plate contact from seismic moment tensors and GPS observations: Tectonophysics, v. 426, p. 295–317, https://doi.org/10.1016/j.tecto.2006.08.004.

Stein, C.A., and Stein, S., 1992, A model for the global variation in oceanic depth and heat flow with lithospheric age: Nature, v. 359, p. 123–129, https://doi.org/10.1038/359123a0.

van Hinsbergen, D.J.J., Vissers, R.L.M., and Spakman, W., 2014, Origin and consequences of western Mediterranean subduction, rollback, and slab segmentation: Tectonics, v. 33, p. 393–419, https://doi.org/10.1002/2013TC003349.

Yuan, X., Kind, R., Li, X., and Wang, R., 2006, The *S* receiver functions: Synthetics and data example: Geophysical Journal International, v. 165, p. 555–564, https://doi.org/10.1111/j.1365-246X.2006.02885.x.

Printed in USA

Downloaded from https://pubs.geoscienceworld.org/gsa/geology/article-pdf/47/3/227/4650237/227.pdf
by Univ de Granada Biblioteca Fac de Ciencias user